

A Dynamical Model for the Coupled Inner Magnetosphere and Tail

Isidoros Doxas, Wendell Horton, WeiTai Lin, Stanley Seibert, and Manish Mithaiwala

Abstract—WINDMI-RC is a family of physics-based models that range in dimensionality from low-order models of dimension $d = 8$, which model the flow of energy between the eight highest global energy components of the tail, to high-order models with dimension $d \sim 100$ or more, for models that resolve the nonlinear dynamics of the system into different latitude zones. The models are intrinsically three-dimensional in configuration space and use the basic geometry of the Tsyganenko magnetic field model to define the geometrical quantities. The models satisfy the constraints of the conservations laws of energy and electrical charge in their network of nodes and branches that follow from the structure of the system. These models describe the injection of plasma from the plasma sheet and across the Alfvén layer into the inner ring current. The transport uses the storm-time solar wind dynamo electric field as the driver for the network model coupled to the inner magnetospheric corotation electric field.

Index Terms—Magnetic storm, magnetosphere, ring current.

I. INTRODUCTION

WINDMI is a physics-based low-dimensional model for the coupled solar wind-magnetosphere-ionosphere system [1], [2] that couples the four basic energy components of the nightside magnetosphere (lobe magnetic energy, plasma thermal energy, parallel kinetic energy, and cross-tail perpendicular kinetic energy [1], [2]) to the ionosphere via the night side region-1 currents. The model is a six-dimensional 13-parameter system, given by

$$L \frac{dI}{dt} = V_{\text{sw}}(t) - V + M \frac{dI_1}{dt} \quad (1)$$

$$C \frac{dV}{dt} = I - I_1 - I_{\text{ps}} - \Sigma V \quad (2)$$

$$\frac{3}{2} \frac{dp}{dt} = \Sigma \frac{V^2}{\Omega_{\text{cips}}} - u_0 K_{\parallel}^{\frac{1}{2}} \Theta(I - I_c) p \quad (3)$$

$$\frac{dK_{\parallel}}{dt} = I_{\text{ps}} V - \frac{K_{\parallel}}{\tau} \quad (4)$$

$$L_I \frac{dI_1}{dt} = V - V_I + M \frac{dI}{dt} \quad (5)$$

$$C_I \frac{dV_I}{dt} = I_1 - \Sigma_I V_I. \quad (6)$$

The quantities L , C , Σ , L_I , C_I , and Σ_I are the magnetospheric and ionospheric inductance, capacitance, and conductance, respectively. M is the mutual inductance. The pressure gradient driven current is given by $I_{\text{ps}} = \alpha p^{1/2}(t)$ as derived from force balance and Ampère's law. The parameter α is an average over the pressure profile in the current sheet. The solar wind driving voltage V_{sw} in (1) is the input time series for this nonlinear driven-dissipative system. The term $u_0 K_{\parallel}^{1/2} \Theta(I - I_c) p$ in (3) represents the rapid unloading of the stored energy when the current exceeds a critical value I_c and comes from the heat flux limit that is neglected in the magnetohydrodynamic (MHD) closure [1]. In the absence of driving ($V_{\text{sw}} = 0$) and damping ($\Sigma_I = 0$), and below the unloading limit ($I < I_c$), the total energy is conserved. All parameters of the model can be calculated explicitly from their integral definitions given the plasma conditions in the tail [1]–[4].

The dynamical system described by (1)–(6) is derived from the Vlasov equation with a heat-flux limit closure scheme [1], [3]. The essential non-MHD physics included in the model is given by the following.

- 1) The collisionless transport for the geomagnetic tail, which appears in the conductivity Σ , transfers energy between (2) and (3). The large ion gyroradius conductivity gives a finite conductance and nonadiabatic ion thermalization in the quasineutral sheet which vanishes in the MHD limit. The conductivity was derived from theory and particle simulations [3], [4] and contains the energization mechanism for the transient ions [7].
- 2) The kinetic loss rate of thermal energy which is described by the parallel heat flux, represented by the heat flux limit parameter u_0 , and the mean parallel flow velocity associated with the MHD parallel flow kinetic energy, K_{\parallel} [(3)]. The Geotail particle data, analyzed with respect to the parallel thermal flux by [8], show that the minimum ratio of the thermal plasma energy density p to the kinetic energy density $(1/2)\rho v^2$ found in the central plasma sheet is consistent with a parallel heat flux q_{\parallel} taken as a fraction of $p v_{\parallel}$, as in (3).

For WINDMI to be used as a forecasting tool, the parameters of the model need to be calculated. This can be done explicitly from the plasma parameters in the tail (density, temperature, etc.) since all WINDMI parameters are defined as integrals of physically identifiable quantities (the capacitance C , for instance, is the volume integral of the $E \times B$ kinetic energy in the current sheet; the unloading parameter u_0 is the surface integral of the heat flux over the boundary, etc). Absent *in situ* data, simulations can also be used to make estimates of the values of these parameters, and this is the avenue that has been pursued so

Manuscript received November 3, 2003; revised February 19, 2004. This work was supported by the National Science Foundation under Grant 0229863.

I. Doxas is with the Center for Integrated Plasma Studies, University of Colorado, Boulder, CO 80309 USA (e-mail: doxas@colorado.edu).

W. Horton, W. Lin, S. Seibert, and M. Mithaiwala are with the Institute for Fusion Studies, The University of Texas, Austin, TX 78712 USA (e-mail: horton@physics.utexas.edu; weitai@mail.utexas.edu; vol-sung@physics.utexas.edu; mithaiwa@mail.utexas.edu).

Digital Object Identifier 10.1109/TPS.2004.833388

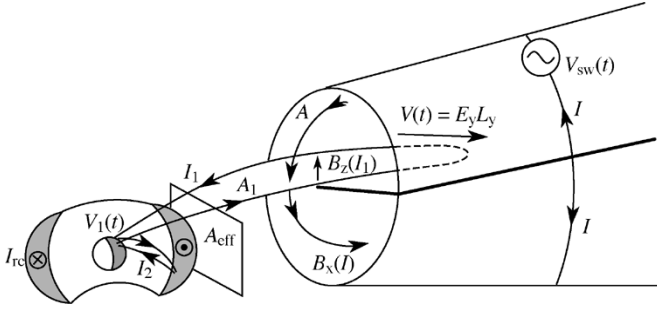


Fig. 1. Schematic of the current systems treated by the model. A_{eff} is the effective area of the aperture presented by the Alfvén layer for the entrance of CPS plasma into the inner magnetosphere [cf., (10)]. I_2 is the partial ring current.

far. Particle simulations are used to provide the moments of the distribution function, which in turn can be used to calculate the parameters of the model using their integral definitions [1]. The output of the model is then compared to well-known datasets (e.g., [9] and [10]). We consistently find that, when using his procedure, WINDMI produces good agreement with observations [11], [12].

Fig. 1 gives the overall geometry of the model, including the ring current and partial ring current which will be addressed in the next section. Although it is tempting to consider WINDMI as a circuit model, it should be noted that (1)–(4) are derived from the closure of the moments of the Vlasov equation (cf., [1] and [2]) and that their circuit-like appearance is a choice of convenience, that allows us to easily extend the model with additional circuit equations, like (5) and (6). In particular, the non-MHD closure scheme adds an energy unloading term [second term on the right-hand side of (3)] which is critical for modeling a class of internally triggered events that cannot be reproduced by load ratio control circuit models (cf., [13]).

In the next section, we will add the ring current to the WINDMI model. In Section III, we will make estimates for the values of some of the model parameters based on the Tsyganenko model. Finally, in Section IV, we will make a connection to existing models like the Burton model [14] and the Temerin–Li model [15].

II. ADDING RING CURRENT ENERGY AND D_{st} TO WINDMI

Consider the magnetosphere as the union (\cup) of the volumes of the lobe Ω_ℓ , the central plasma sheet Ω_{cps} , the small transition (Alfvén) volume Ω_{tr} surrounding the separatrix between the inner ring current and the outer magnetospheric plasma, and the volume of the ring current itself Ω_{rc} . The volume of the magnetosphere is then $\Omega_{\text{MAG}} = \Omega_{\text{rc}} \cup \Omega_{\text{tr}} \cup \Omega_{\text{cps}} \cup \Omega_\ell$. Now, the total plasma energy is decomposed as $W_p = \sum_\alpha \int_{\Omega_\alpha} d^3x (3/2)p = (3/2)p_{\text{cps}}\Omega_{\text{cps}} + (3/2)p_{\text{rc}}\Omega_{\text{rc}}$, since the particle pressure is negligible in the lobe plasma and the transition layer volume is a small fraction of Ω_{cps} . The Dessler–Parker relation [16], [17] gives the D_{st} index through the total ring current energy $W_{\text{rc}}(t) = (3/2)\Omega_{\text{rc}}p_{\text{rc}}$. The principal source of $W_{\text{rc}}(t)$ is the plasma flux from the central plasma sheet $p_{\text{cps}}v_x$.

The Dessler–Parker relation

$$\frac{\Delta B_{\text{particles}}}{B_E} = -\frac{\mu_0}{2\pi} \frac{W_{\text{rc}}}{B_E^2 R_E^3} \quad (7)$$

is used for the physics modeling to give the ring current plasma energy $W_{\text{rc}}(t)$ from the ΔB_z at the magnetometers used for the D_{st} magnetic index. Thus, the ring current $I_{\text{rc}}(t)$ and the associated induction electric field $E_{\text{rc}}(t)$ from the ring current inductance are conjugate variables for the inner magnetosphere electrodynamics. In (7), $B_E = 3.1 \cdot 10^{-5}$ T is the magnetic field strength of the Earth’s internal dipole field at the Earth’s surface on the equator.

Both protons and electrons can acquire large amounts of energy as they drift Earthward in the dynamical magnetotail during the storms. The Lorentz force gives the exact orbits of the particle motions $\mathbf{F}_L = q(\mathbf{E} + \mathbf{v} \times \mathbf{B})$. Averaging over the cyclotron gyrations gives the approximate guiding center orbit equations. The duskward electric field is time and space varying due to the time variation of the solar wind and the projection of the E_y vector on the plane perpendicular to the local magnetic field. This projection is important to give zero parallel electric field, and the physics of this process is that the first-order electrons move to cancel the parallel component of the dynamo electric field.

The fractional diversion of the particles across the separatrix formed by the corotation electrostatic field and the storm time varying convection electric field can be considered as a scattering and trapping problem for ensembles of electron and ion kappa distributions. Such a process can then be modeled by an effective admission cross-section A_{eff} for the fraction of the particles that cross the separatrix. Of course, this fraction depends on the nature of the storm time electric field and the state of the transitional region of the transitional magnetic field so only a rough characterization of the trapping fraction is possible from theory. The parameter A_{eff} is then one of the more critical parameters of the model and can be either estimated from theory (e.g., by Monte Carlo simulations) or viewed as a parameter to be optimized. A schematic of the ring current and its position relative to the other currents in the model is shown in Fig. 1. The effective aperture A_{eff} is shown schematically as the cross section that some fraction of the plasma sheet particles will cross in order to populate the ring current.

We integrate the Poynting flux over the toroidal volume Ω_{rc} with the aperture A_{eff} in the midnight sector of its surface $\partial\Omega_{\text{rc}}$ to obtain

$$\frac{\partial}{\partial t} \int_{\Omega_{\text{rc}}} \left(\frac{1}{2} \rho v_E^2 + \frac{B^2}{2\mu_0} + p_\perp \right) d^3x = \int_{A_{\text{eff}}} p v_{xE} \cdot da - \int_{\Omega_{\text{rc}}} \mathbf{j}_{\text{gc}} \cdot \mathbf{E} d^3x \quad (8)$$

where \mathbf{j}_{gc} is the guiding drift current density and v_E the $\mathbf{E} \times \mathbf{B}$ drift velocity. To derive the energy density in (8) that contains the $\mathbf{E} \times \mathbf{B}$ flow and the plasma pressure, the microscopic form of the Poynting theorem is transformed with $\mathbf{j} = (\rho/B^2)(d\mathbf{E}_\perp/dt) + \nabla \times \mathbf{M} + \mathbf{j}_{\text{gc}}$, where ρ is the mass density and $\mathbf{M} = -p_\perp \mathbf{B}/B^2$ the magnetization. Both polarization and magnetization currents arise from the gyro orbits. The power $\int \mathbf{j}_{\text{gc}} \cdot \mathbf{E} d^3x$ is the sum of: 1) the energization of the plasma by the convection electric field outside the

separatrix where $\Delta P_{\text{gc}} = \int \mathbf{j}_{y,\text{gc}} E_y d^3x = I(t)V(t)$ and 2) the energization of the ring current particles

$$\frac{dW_{\text{rc}}}{dt} = \int \mathbf{j}_{\text{rc}} \cdot \mathbf{E} d^3x = I_{\text{rc}}(t)\Delta V_{\text{rc}} \quad (9)$$

inside the separatrix, where ΔV_{rc} is the electromotive potential across the foot points of the partial ring current.

The ring current energization \dot{W}_{rc} can be rewritten in the form of the power expended in moving those particles inward up against the expansion force $\mathbf{F} = -(p_{\perp}/B)\nabla B - p_{\parallel}\boldsymbol{\kappa}$ where $\boldsymbol{\kappa} = (\hat{\mathbf{b}} \cdot \nabla)\hat{\mathbf{b}}$ is the magnetic curvature. This follows after we observe that $\mathbf{j}_{\text{gc}} \cdot \mathbf{E} = \sum_{\text{rc}}(\mathbf{F} \times \mathbf{B}/B^2) \cdot \mathbf{E} = -\sum \mathbf{v}_E \cdot \mathbf{F} \cong -v_x \mathbf{F}_x$ is the work done by the external worker—here the central plasma sheet—to compress the plasmas into the ring current. For an inward motion Δx we integrate, with the approximation of constant p_{\perp}/B and $p_{\parallel}\boldsymbol{\kappa}_x$, to get $\Delta W_{\text{rc}} = (p_{\perp}/B)(B_f - B_i) + p_{\parallel}(\Delta x/R_c)$.

Thus, the projection of the relevant partial differential equations and atomic physics onto the ring current energy balance equation gives the ordinary differential equation

$$\frac{dW_{\text{rc}}}{dt} = I_{\text{rc}}(t)\Delta V_{\text{rc}} + \frac{p_{\text{cps}}(t)V(t)A_{\text{eff}}}{B_{\text{tr}}L_y} - \frac{W_{\text{rc}}}{\tau_{\text{rc}}} \quad (10)$$

where τ_{rc} is the decay time which is dominated by charge exchange [18] (see estimates in Section III), and $V(t)A_{\text{eff}}/L_y B_{\text{tr}}$ is the injection from the dawn-to-dusk potential drop in the central plasma sheet. A_{eff} is the area of the aperture presented by the Alfvén layer for the entrance of CPS plasma into the inner magnetosphere for the particular storm. We discuss the modeling of this aperture in Section III. Clearly, the aperture is varying during a storm, so using an average value is a first-step model.

Including the equation for the I_2 current loop together with (10) into the WINDMI model, we obtain

$$L \frac{dI}{dt} = V_{\text{sw}}(t) - V + M \frac{dI_1}{dt} \quad (11)$$

$$C \frac{dV}{dt} = I - I_1 - I_{\text{ps}} - \Sigma V \quad (12)$$

$$\frac{3}{2} \frac{dp}{dt} = \frac{\Sigma V^2}{\Omega_{\text{cps}}} - u_0 K_{\parallel}^{\frac{1}{2}} \Theta(I - I_c)p - \frac{pV A_{\text{eff}}}{\Omega_{\text{cps}} B_{\text{tr}} L_y} \quad (13)$$

$$\frac{dK_{\parallel}}{dt} = I_{\text{ps}}V - \frac{K_{\parallel}}{\tau} \quad (14)$$

$$L_I \frac{dI_1}{dt} = V - V_I + M \frac{dI}{dt} \quad (15)$$

$$C_I \frac{dV_I}{dt} = I_1 - I_2 - \Sigma_I V_I \quad (16)$$

$$L_2 \frac{dI_2}{dt} = V_I - (R_{\text{prc}} + R_{A2})I_2 \quad (17)$$

$$\frac{dW_{\text{rc}}}{dt} = R_{\text{prc}}I_2^2 + \frac{pV A_{\text{eff}}}{B_{\text{tr}}L_y} - \frac{W_{\text{rc}}}{\tau_{\text{rc}}} \quad (18)$$

where the D_{st} signal is given by

$$D_{\text{st}} = -\frac{\mu_0 W_{\text{rc}}(t)}{2\pi B_E R_E^3}. \quad (19)$$

Here, L_2 is the inductance of the region 2 current loop, and R_{prc} and R_{A2} are the resistances of the partial ring current and the region 2 foot point in the auroral region. The system of (11)–(18) is the WINMDI-RC model, a $d = 8$ system of equations for the solar wind-driven coupled inner magnetosphere, ionosphere, and tail. Together with (19), the model gives a prediction of the D_{st} index while conserving energy in the coupled inner magnetosphere–tail system. Here, we conclude with the following estimates and observations.

From the model [19] of the R1-R2 auroral coupling region, we infer nominal-to-maximum currents and voltages as $I_1 \sim 1$ MA, $I_2 \sim 500$ kA, $V_I \sim 100$ kV, and $R_{\text{prc}}I_2 \simeq 50$ kV – 100 kV so that the partial ring current energization power is of order 25–50 GW [20] and gives an estimate of combining Region 1 and Region 2 currents of 300 GW so that 30 GW would only be 10% of the Stern’s power estimate.

The CPS injection is highly dependent on the dynamical activity in the geomagnetic tail. Nonetheless, we may estimate bounds and an average value for the aperture. For $A_{\text{eff}} = R_E^2 = 3.6 \times 10^{13} \text{ m}^2$ with $p_{\text{cps}} \sim 5$ nPa and $v_x = 100$ km/s the flux for injection into the inner magnetosphere is $p v_x = 5 \times 10^{-4} \text{ W/m}^2$ with $P_{\text{inj}} \sim 20$ GW. With A_{eff} growing to $10R_E^2$ there are 200 GW entering the inner magnetosphere. We discuss methods known for calculating the injection process in detail in the next section.

III. TSYGANENKO RING CURRENT AND TAIL CURRENT

A detailed version of the Dessler–Parker relation follows from Tsyganenko’s model using an analytic expression for the ring current vector potential A_{ϕ} , in cylindrical coordinates, where $\rho = (X_{\text{gsm}}^2 + Y_{\text{gsm}}^2)^{1/2}$ is the radial distance, and ϕ is the angle about the z axis and corresponds to the longitude. The model for $A_{\phi} = C\rho/(\rho^2 + z^2 + 4\rho_0^2)^{3/2}$ produces a well-localized current distribution centered at ρ_0 and decreasing as $(\rho_0/\rho)^6$ for $\rho \gg \rho_0$. Clearly, the model applies for $(\rho^2 + z^2)^{1/2} \gg R_E$ and neglects the noon–midnight asymmetry. We know Tsyganenko’s parameterization of the constants C and ρ_0 as a function of K_p . We determine the total ring current through $\mu_0 I_{\text{rc}} = C/\rho_0^2$ and the stored energies W_{rc} and W_{rc}^B , where W_{rc}^B is the magnetic energy stored in the ring current. Parameter values were given through a maximum value of $K_p = 5$ in [21]; for this paper, we extended these values using a linear fit through a maximum value of $K_p = 9$. We can calculate the magnetic field according to $\mathbf{B} = \text{curl} A_{\phi} \hat{\boldsymbol{\phi}} = \nabla(\rho A_{\phi}) \times \nabla\phi$ and determine the $\Delta B_z(\rho = R_E, z = 0)$ for the model D_{st} . The contribution of the geotail current to the D_{st} is approximately 20%–25% according to [22].

The current distribution of the ring current may be obtained from the vector potential of (8), by $\mathbf{J} = -1/\mu_0 \nabla^2 \mathbf{A}$ since $\nabla \cdot \mathbf{A} = 0$. The ring current density is

$$J_{\phi} = \frac{60I_{\text{rc}}(t)\rho_0^4}{(\rho^2 + z^2 + 4\rho_0^2)^{\frac{5}{2}}}. \quad (20)$$

TABLE I
WINDMI PARAMETERS

		$u_0 (4.2 \times 10^{-9}) / \text{m/kg}^{1/2}$	Heat flux limit parameter for parallel thermal flux on open magnetic field lines $q_{\parallel} = u_0(K_{\parallel}/\rho_m)^{1/2}$ where $(K_{\parallel}/\rho_m)^{1/2}$ is the mean parallel flow velocity.
V^{sw}	Solar wind input voltage from interplanetary electric field $V_x^{\text{sw}}B_s$ and effective magnetopause interaction length L_y^{eff} . $V^{\text{sw}} = V_x^{\text{sw}}B_sL_y^{\text{eff}}$ in volts.	τ (10 min)	Confinement time for the parallel flow kinetic energy K in the central plasma sheet.
L (97.4 H)	Inductance of the lobe cavity surrounded by the geotail current $I(t)$. The nominal value is $L = \mu_0 A_{\ell} / L_x^{\text{eff}}$ in Henries where A_{ℓ} is lobe area and L_x^{eff} the effective length of the geotail solenoidal. Computation of L as function of the IMF from Tsyganenko are given in [2].	$I(p)$	The geotail current driven by the plasma pressure p confined in the central plasma sheet. Pressure balance between the lobe and the central plasma sheet gives $B_{\ell}^2/2\mu_0 = p$ with $2L_x B_{\ell} = \mu_0 I_p$. This defines the coefficient α in $I_p = \alpha(p)^{1/2}$ to be approximately $\alpha = 2.8L_x/\mu_0^{1/2}$.
C (48000 F)	Capacitance of the central plasma sheet in Farads. The nominal value is $C = \rho_m L_x L_z / B^2 L_y$ where ρ_m is the mass density in kg/m^3 , $L_x L_z$ is the meridional area of the plasma sheet, L_y the dawn-to-dusk width of the CPS and B the magnetic field on the equatorial plane. Computations of C are given in [1].	L_1 (19 H)	The self-inductance of the wedge current or the nightside region 1 current loop $I_1(t)$
		M (2/3 H)	The mutual inductance between the nightside region 1 current loop I_1 and the geotail current loop I .
		L_2 (8H)	The inductance of the ring current.
		C_1 (800 F)	The capacitance of the nightside region 1 plasma current loop.
Σ (7.8 mho)	Large gyroradius ρ_i plasma sheet conductance from the quasineutral layer of height $(L_z \rho_i)^{1/2}$ about the equatorial sheet. The nominal value of $\Sigma = 0.1(n_e/B_n)(\rho_i/L_z)^{1/2}$. Computation of Σ is given in [1].	Σ_I (3 mho)	The ionospheric Pedersen conductance of the westward electrojet current closing the I_1 current loop in the auroral (~ 100 km, 68°) ionosphere.
		R_{prc} (0.1 ohm)	The resistance of the partial ring current.
Ω (10000 R_E^3)	Volume of the central plasma sheet that supports mean pressure $p(t)$. In some works $\Omega = \Omega_{\text{cps}}$.	τ_{rc} (12 hrs)	The decay time for the ring current energy.
		A_{eff} ($2R_E^2$)	The effective area presented to the geotail plasma for plasma entry into the innermagnetosphere.

The maximum of the current density is located at $\rho_{\text{max}} = \sqrt{2/3}\rho_0$, $z = 0$, which occurs at about $4.2R_E$ for $K_p = 0$ and decreases to $2.5R_E$ for $K_p = 9$.

From the value for B_z evaluated at $\rho = R_E$, we see that the relationship between the current and the D_{st} index is $D_{\text{st}} = \mu_0 I_{\text{rc}} / (4\rho_0)$. For the reference values of $I_{\text{rc}} = 4$ MA and $\rho_0 = 4.9R_E$, this gives $D_{\text{st}} = -40$ nT.

The magnetic energy W_{rc}^B , stored in the ring current, is given by $W_{\text{rc}}^B = 1/2 \int \mathbf{J} \cdot d\mathbf{A}$. Using (20), we obtain $W_{\text{rc}}^B = (5/512)\mu_0 \rho_0 I_{\text{rc}}^2$. The magnetic energy and the D_{st} index are therefore related by $D_{\text{st}} = (512\mu_0/20\pi^2 C)W_{\text{rc}}^B$, where $C = I_{\text{rc}}\pi\rho_0^2$. The self-inductance of the ring current is given by $L_{\text{rc}} = 2W_{\text{rc}}^B/I_{\text{rc}}^2$. Using $I_{\text{rc}} = C/\pi\rho_0^2$ and W_{rc}^B gives the inductance $L_{\text{rc}} = 5\pi^2/256\mu_0\rho_0 \simeq 8$ H at $\rho_{\text{max}} = 4.2R_E$. For comparison, the inductance of a tokamak is $L = \mu_0 R [\log(R/a) + 1/4]$, where R is the major radius and a is the minor radius. Applying the formula to the ring current with $R = 4R_E$ and $a = 2R_E$ gives an approximation for the inductance of the ring current of about $L_{\text{rc}} = 8$ H. The effect of the large aspect ratio approximation is that the inductance

scales logarithmically with respect to the aspect ratio R/a of the current profile model.

For the model equations, it is important to know the self-inductance L_{rc} of the ring current. We have computed the total ring current I_{rc} , the total magnetic energy W_{rc}^B from I_{rc} , and the self-inductance from the Tsyganenko magnetic field model as a function of the D_{st} . We see that for $D_{\text{st}} = -40$ nT, we have $L_{\text{rc}} = 8$ H, and $I_{\text{rc}} = 4$ MA, so that $W_{\text{rc}}^B = 6 \times 10^{12}$ J.

The summation of all the energy loss processes is thought to be dominated by charge exchange losses on the O^+ and H^+ from the atmosphere [18] with $\tau_{\text{rc}} \sim 1/2$ day = 4.32×10^4 s. The stored ring current energy from (18) at equilibrium would be $W_{\text{rc}} = (P_2 + P_A)\tau_{\text{rc}} = 25 \text{ GW} \times 8.64 \times 10^4 \text{ s} = 3.5 \times 10^{15}$ J. Thus, $W_{\text{rc}} \gg W_{\text{rc}}^B$ so that the estimate of the plasma energy appears high from the point of view of laboratory MHD equilibrium and stability.

Table I lists the parameters of the model, with estimates of typical values. Fig. 2 shows the results of the WINDMI-RC model for the storm of May 15, 1997. The values of the model parameters used in that particular simulation are given in paren-

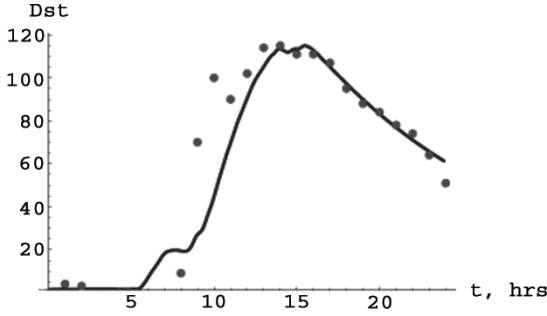


Fig. 2. D_{st} index (heavy line) and the WINDMI-RC response (dots) for the storm of May 15, 1997. Value of effective aperture is $A_{eff} = 7.7 \times 10^{14} / (B_{tr} L_y)$ [cf., (18)], which corresponds to $A_{eff} = 2.0 R_E^2$.

thesis in Table I. We see that the model gives good agreement with observations for reasonable values of the parameters.

IV. CONNECTION TO EXISTING MODELS

Equations (11)–(19) should be compared with the Burton equation [14] and a recent extension of the Burton equation due to [15]. The [14] formulation gives the D_{st} as

$$D_{st} = D_{st}^{rc} + b\sqrt{p_{dyn}} - c. \quad (21)$$

The D_{st} is a sum of three terms: the contribution from the ring current, the contribution from the magnetopause current, which is dependent on the dynamic pressure p_{dyn} , and the quiet condition represented by c . The ring current contribution to the D_{st} , D_{st}^{rc} is

$$\frac{d}{dt} D_{st}^{rc} = F(E_{sw}) - a D_{st}^{rc} \quad (22)$$

where $F(E_{sw})$ is the injection of energy into the ring current which depends on the solar wind electric field E_{sw} , and a is the inverse decay time of the ring current. Equations (21) and (22) can be combined to give the total change of the D_{st} which is known as the Burton equation.

The Temerin–Li formulation represents the D_{st} as a sum of several terms

$$D_{st} = d_{st}^1 + d_{st}^2 + d_{st}^3 + \text{Pressure Term} + f(B_z^{IMF}) C. \quad (23)$$

The *pressure term* is not given only by $\sqrt{p_{dyn}}$ as in the [14] formulation, but includes a dependence on the solar wind density. The three terms d_{st}^t are introduced empirically where d_{st}^1 represents the ring current contribution as done by Burton and $d_{st}^2 + d_{st}^3$ “probably represents some combination of the so-called partial ring current and the tail currents” [15]. The key new physics in the WINDMI-RC model is the effective aperture A_{eff} , which will need to be parametrized in terms of B_z^{IMF} , similar to the $f(B_z^{IMF})$ term in (23).

V. CONCLUSION

A dynamical model of the coupled inner magnetosphere tail has been constructed by considering the coupling of the ring current energy to the central plasma sheet and using the Dessler–Parker relation to compute the D_{st} from the ring

current energy. The effective aperture A_{eff} for transferring energy from the CPS through the Alfvén separatrix layer to the ring current can be either estimated or used as a parameter to be optimized.

The major advantage of this proposed model is that the separate components of the magnetospheric current system, such as the ring current, tail current, and partial ring current, are introduced explicitly and not in an empirical manner. It is important to determine the relative contributions of these systems to the total D_{st} . For example [22], determine the contribution from the tail current to be approximately one-quarter of the total D_{st} .

The key advantage of the physics-derived energy and charge-conserving models is that the flow of energy can be tracked and cataloged for different types and strengths of storms. It may well be that the models will give a useful intermediate level tool for interpreting (ordering) storm data. Contracting a large storm observational database to a smaller physically ordered database would be of considerable benefit to MHD modelers.

REFERENCES

- [1] W. Horton and I. Doxas, “A low dimensional energy conserving state space model for substorm dynamics,” *J. Geophys. Res.*, vol. 101A, p. 27223, 1996.
- [2] —, “A low dimensional dynamical model for the solar wind driven geotail-ionosphere system,” *J. Geophys. Res.*, vol. 103A, p. 4561, 1998.
- [3] W. Horton and T. Tajima, “Collisionless conductivity and stochastic heating of the plasma sheet in the geomagnetic tail,” *J. Geophys. Res.*, vol. 96, p. 15811.
- [4] —, “Transport from chaotic orbits in the geomagnetic tail,” *Geophys. Res. Lett.*, vol. 18, p. 1583.
- [5] T. Lefschetz and T. Solomon, *Applications of Algebraic Topology: Graphs and Networks: The Picard=Lefschetz Theory and Feynman Integrals*. New York: Springer-Verlag, 1975, p. 189.
- [6] P. Bamber and S. Sternberg, *A Course in Mathematics for Students of Physics*. Cambridge, MA: Cambridge Univ. Press, 1990, p. 474.
- [7] L. R. Lyons and T. W. Speiser, “Evidence for current sheet acceleration in the geomagnetic tail,” *J. Geophys. Res.*, vol. 87, p. 2276, 1982.
- [8] M. Hoshino, T. Mukai, and T. Yamamoto, “Ion dynamics in magnetic reconnection: Comparison between numerical simulations and Geotail observations,” *J. Geophys. Res.*, vol. 103, p. 4509, 1998.
- [9] G. T. Blanchard and R. L. McPherron, “A bimodal representation of the response function relating the solar wind electric field to the AL index,” *Adv. Space Res.*, vol. 13, p. 71, 1993.
- [10] L. F. Bargatze, D. N. Baker, R. L. McPherron, and E. W. Hones, “Magnetospheric impulse response for many levels of geomagnetic activity,” *J. Geophys. Res.*, vol. 90, p. 6387, 1985.
- [11] I. Doxas, W. Horton, and J. P. Smith, “A physics based nonlinear dynamical model for the solar wind driven magnetosphere-ionosphere system,” *Phys. Chem. Earth*, vol. 24, p. 67, 1999.
- [12] I. Doxas, W. Horton, and R. Weigel, “Using particle simulations for parameter tuning of dynamical models of the magnetotail,” *J. Astrophys. Solar-Terrestrial Phys.*, vol. 64, p. 633, 2002.
- [13] R. S. Weigel, W. Horton, and I. Doxas, “Substorm classification with the WINDMI model,” *Nonlinear Processes Geophys.*, vol. 10, p. 363, 2003.
- [14] R. K. Burton, R. L. McPherron, and C. T. Russel, “An empirical relationship between interplanetary conditions and D_{st} ,” *J. Geophys. Phys.*, vol. 80, p. 4204, 1975.
- [15] M. Temerin and X. Li, “A new model for the prediction of D_{st} on the basis of the solar wind,” *J. Geophys. Phys.*, vol. 107, p. 1472, 2002.
- [16] A. J. Dessler and E. N. Parker, “Hydromagnetic theory of geomagnetic storms,” *J. Geophys. Res.*, vol. 64, p. 2239, 1959.
- [17] N. Sckopke, “A general relation between the energy of trapped particles and the disturbance field near the Earth,” *J. Geophys. Res.*, vol. 71, p. 3125, 1966.
- [18] M. W. Chen and M. Schulz, “Ring current formation and decay: A review of modeling work,” in *Advances in Space Research*. London, U.K.: Elsevier, 1996, vol. 17, pp. 7–16.
- [19] G. L. Siscoe, “Energy coupling between regions 1 and 2 Birkeland current systems,” *J. Geophys. Res.*, vol. 87, no. A7, p. 5124, 1982.

- [20] D. P. Stern, "The beginning of substorm research," in *Magnetospheric Substorms*, J. R. Kan, T. A. Potemra, S. Kokubun, and T. Iijima, Eds. Washington, DC: Amer. Geophys. Union, 1991, p. 11.
- [21] N. A. Tsyganenko, "Global quantitative models of the geomagnetic field in the cislunar magnetosphere for different disturbance levels," *Planet. Space Sci.*, vol. 35, p. 1347, 1987.
- [22] N. E. Turner, D. N. Baker, T. I. Pulkkinen, and R. L. McPherron, "Evaluation of the tail current contribution to D_{st} ," *J. Geophys. Res.*, vol. 105, pp. 5431–5439, 2000.



Isidoros Doxas is a Senior Research Associate at the University of Colorado, Boulder, and a Fellow at the Center for Integrated Plasma Studies. He has worked on plasma turbulence in laboratory and space plasmas, stochastic transport in fusion devices, quasi-linear theory, and magnetospheric physics.



Wendell Horton is a Professor of Physics at the University of Texas, Austin, and a Research Scientist at the Institute for Fusion Studies. His research interests include plasma transport, on which he has published a wide range of scientific works ranging from the fundamental symmetries in collisional and turbulent transport equations to exotic soliton wave transport mechanics.

WeiTai Lin received the B.S. degree from the National Central University, Taiwan, R.O.C., and the M.S. degree in electric engineering from the University of Texas, Austin, in 2003.



Stanley Seibert received the B.S. degree in physics and computer science from Arizona State University, Tempe, in 2002. He is working toward the Ph.D. degree in physics at the University of Texas, Austin, performing research in solar neutrino physics.



Manish Mithaiwala received the B.S. degrees in physics and mathematics from the University of Illinois, Urbana–Champaign. He is currently working toward the Ph.D. degree at the University of Texas, Austin.

His research interests include simulations involving space/astrophysical plasmas, space plasma instabilities, and problems in nonlinear plasma physics.